

Active Sensing Control for Differentially Flat Systems

Olga Napolitano¹, *Student Member, IEEE*, Annamaria Pinizzotto², Matteo Verdecchia³,
Alessio Pettinari⁴, Daniela Selvi⁵, Lucia Pallottino⁶, *Senior Member, IEEE*,
and Paolo Salaris⁷, *Member, IEEE*

Abstract—This letter proposes an optimal active perception strategy using the *Constructibility Gramian (CG)* as a metric to quantify the richness of the information acquired along the planned trajectory. A critical issue is the dependence of the CG on the transition matrix, whose closed-form expression is not available for most robotic systems while its numerical computation is usually costly. We leverage differential flatness to transform the nonlinear system in the Brunovsky form, for which the transition matrix reduces to the exponential of a Jordan block. The resulting CG is a measure of the acquired information through the flat outputs about the flat outputs themselves and their derivatives. The inverse flatness change of coordinates is then used to come back to the original state variables, needed for computing the feedback control law. The flat outputs are parameterized through B-Splines with control points determined by actively maximizing CG. We simulate our approach on a unicycle vehicle and a planar UAV that need to estimate their configuration while measuring their distance w.r.t. two fixed markers. Simulations show the effectiveness of our methodology in reducing both the computational time and the estimation uncertainty.

Index Terms—Optimization, robotics, information theory and control.

I. INTRODUCTION

TO MOVE autonomously in unknown environments, robots are required to continuously estimate their own state and reconstruct the surroundings space. To this aim, the sensing data provided by onboard sensors and (possibly) in the environment can be exploited. In nonlinear frameworks, such as the ones of interest in robotic applications, the possibility

Manuscript received 8 March 2024; revised 18 May 2024; accepted 9 June 2024. Date of publication 14 June 2024; date of current version 10 July 2024. This work was supported in part by the European Union's Horizon 2020 Research and Innovation Programme, (DARKO) under Grant 101017274; in part by the European Union by the Next Generation EU, Ecosistema dell'Innovazione Tuscany Health Ecosystem (THE, PNRR, Spoke 9: Robotics and Automation for Health) under Project ECS00000017; and in part by the Italian Ministry of Education and Research (MIUR) in the Framework of the CrossLab and ForeLab Project (Departments of Excellence). Recommended by Senior Editor S. Dey. (Annamaria Pinizzotto, Matteo Verdecchia, Alessio Pettinari, and Daniela Selvi contributed equally to this work.) (Corresponding author: Paolo Salaris.)

The authors are with the Research Center "E. Piaggio" and the Department of Information Engineering, University of Pisa, 56122 Pisa, Italy (e-mail: olga.napolitano@phd.unipi.it; daniela.selvi@unipi.it; lucia.pallottino@unipi.it; paolo.salaris@unipi.it).

Digital Object Identifier 10.1109/LCSYS.2024.3414968

of reconstructing the system state based on the available sensor data may depend also on the applied inputs [1], [2]; in some particular cases, the state variables may even be either reconstructable or not, depending on the chosen inputs [3]. Further, among the inputs that allow reconstructing the system state, it is important to determine the ones providing the *maximum* information gathered along the resulting trajectory (or, equivalently, the *minimum* estimation uncertainty). This is particularly important since sensor data are unavoidably affected by noise that corrupts the available information. The problem of action selection in this context is known as *active sensing/perception*, which has been motivating the rise of different strategies within many applications in several robotic fields see, e.g., [4], [5], [6]. Efficient active sensing strategies pass through the selection of a *metric* that quantifies the gathered information. Examples in the literature include the entropy [7], the mutual information [8], Bayesian optimization [9], and finally the Fisher Information Matrix (FIM) [10] and the Constructibility Gramian (CG) [11]. Further approaches are based on Partially Observable Markov Decision Processes and Sequential Decision Processes [12]. Recent works have addressed the active sensing problem with limited sensors and intermittent measurements [13], and in the presence of both measurement and actuation/process noise [14]. In this letter, we adopt the CG as the information metric. However, the CG depends on the transition matrix, whose closed-form expression is usually not available, and whose numerical evaluation can rapidly become computationally costly. To overcome this issue, the differential flatness property can be exploited to transform the nonlinear system in the Brunovsky form. Such representation is appealing in our context, as the transition matrix reduces to the exponential of a Jordan block, which is thus available in closed form, therefore reducing the computational cost. The flatness property has been extensively used in the literature for control and state estimation purposes [15], [16]. Among the benefits provided by the flatness, it is worth highlighting that a state estimation algorithm based on the feedback linearized system relies on a *linear* process model; additionally, when the flat outputs can be directly measured by the available sensors [17], [18], the measurement model is linear as well. In both cases, this results in improved performance in terms of accuracy and computational complexity compared to estimation algorithms that rely

on nonlinear models [19]. Based on the above discussion, the contributions of this letter are: i) enhancement of any CG-based active sensing strategy through the transformation of a nonlinear system in the Brunovsky form, ii) introduction of a novel inverse flatness change of coordinates to come back to the CG of the original state variables and iii) reduced computational time in finding an optimal solution to the active sensing problem. We show the effectiveness of our approach on a unicycle vehicle and a planar quadrotor, comparing with random paths and [11].

II. PRELIMINARIES

We consider a robotic system described through the generic nonlinear model

$$\dot{\mathbf{q}}(t) = \mathbf{f}(\mathbf{q}(t), \mathbf{u}(t)), \quad \mathbf{q}(t_0) = \mathbf{q}_0 \quad (1)$$

$$\mathbf{z}(t) = \mathbf{h}(\mathbf{q}(t)) + \boldsymbol{\mu}(t) \quad (2)$$

where $\mathbf{q}(t) \in \mathbb{R}^n$ is the state of the system to be estimated, $\mathbf{u}(t) \in \mathcal{U} \subseteq \mathbb{R}^m$ is the control input, and $\mathbf{z}(t) \in \mathbb{R}^p$ represents the measurements provided by the available sensors; further, \mathbf{f} and \mathbf{h} are analytic functions, and $\boldsymbol{\mu}(t) \sim \mathcal{N}(0, \mathbf{R}(t))$ is a Gaussian noise with zero mean and covariance matrix $\mathbf{R}(t)$. We assume that the system is subject to negligible actuation/process noises. In [11], an online active sensing control strategy has been proposed that relies on the CG as the tool for expressing the ability to retrieve information about the final state \mathbf{q}_f at time t_f from the collected input and output data. We recall that, for any $t_0 < t_f$, the CG [11] is defined as

$$\mathcal{G}_c(t_0, t_f) \triangleq \int_{t_0}^{t_f} \boldsymbol{\Phi}(\tau, t_f)^T \mathbf{H}(\tau)^T \mathbf{W}(\tau) \mathbf{H}(\tau) \boldsymbol{\Phi}(\tau, t_f) d\tau, \quad (3)$$

where $\mathbf{H}(\tau) = \frac{\partial \mathbf{h}(\mathbf{q}(\tau))}{\partial \mathbf{q}(\tau)}$, and $\mathbf{W}(\tau) \in \mathbb{R}^{p \times p}$ is a symmetric positive definite weight matrix that may be used, for example, to account for the reliability of outputs affected by different noise levels. Matrix $\boldsymbol{\Phi}(t, t_f) \in \mathbb{R}^{n \times n}$, known as *sensitivity matrix* of the state trajectory w.r.t. the final conditions \mathbf{q}_f , is defined as $\boldsymbol{\Phi}(t, t_f) = \frac{\partial \mathbf{q}(t)}{\partial \mathbf{q}_f}$ and obeys the following differential equation with *final* conditions at t_f

$$\dot{\boldsymbol{\Phi}}(t, t_f) = \frac{\partial \mathbf{f}(\mathbf{q}(t), \mathbf{u}(t))}{\partial \mathbf{q}(t)} \boldsymbol{\Phi}(t, t_f), \quad \boldsymbol{\Phi}(t_f, t_f) = \mathbf{I}. \quad (4)$$

By the semigroup property, for which $\boldsymbol{\Phi}(t_0, t_f) = \boldsymbol{\Phi}(t_0, \tau) \boldsymbol{\Phi}(\tau, t_f) = \boldsymbol{\Phi}^{-1}(\tau, t_0) \boldsymbol{\Phi}(\tau, t_f)$, it is easy to show that CG is related to the Observability Gramian $\mathcal{G}_o(t_0, t_f)$ as $\mathcal{G}_c(t_0, t_f) = \boldsymbol{\Phi}^T(t_0, t_f) \mathcal{G}_o(t_0, t_f) \boldsymbol{\Phi}(t_0, t_f)$ [11]. In the following, if needed, we will explicitly mention the state variables the CG refers to, e.g., ${}^q\mathcal{G}_c(t_0, t_f)$, is the CG related to the system expressed with state variables \mathbf{q} . We conclude by showing an important link between the CG and the optimal error covariance matrix \mathbf{P} for the Linear Time-Varying (LTV) system obtained by linearizing (1)-(2) around a nominal trajectory $(\mathbf{q}(t), \mathbf{u}(t))$

$$\begin{aligned} \dot{\mathbf{q}}(t) &= \mathbf{A}(t) \mathbf{q}(t) + \mathbf{B}(t) \mathbf{u}(t), \quad \mathbf{q}(t_0) = \mathbf{q}_0 \\ \mathbf{z}(t) &= \mathbf{H}(t) \mathbf{q}(t) + \boldsymbol{\mu}(t) \end{aligned} \quad (5)$$

where $\mathbf{A}(t) = \frac{\partial \mathbf{f}(\mathbf{q}, \mathbf{u})}{\partial \mathbf{q}}$, $\mathbf{B}(t) = \frac{\partial \mathbf{f}(\mathbf{q}, \mathbf{u})}{\partial \mathbf{u}}$ and $\mathbf{H}(t) = \frac{\partial \mathbf{h}(\mathbf{q})}{\partial \mathbf{q}}$. In the absence of process noise, the CG with $\mathbf{W}(t) = \mathbf{R}^{-1}(t)$ for (5)

coincides with the inverse of matrix $\mathbf{P}(t)$, i.e., the optimal covariance matrix associated to the estimation error of the LTV system computed by solving the Riccati equation [20], [21]. Indeed, with $\mathbf{P}_0 = \mathbf{P}(t_0)$, the following holds (see [11])

$$\begin{aligned} \mathbf{P}^{-1}(t) &= \boldsymbol{\Phi}^T(t_0, t) \mathbf{P}_0^{-1} \boldsymbol{\Phi}(t_0, t) + \mathcal{G}_c(t_0, t) \\ &= \boldsymbol{\Phi}^T(t_0, t) \mathcal{G}_c(-\infty, t_0) \boldsymbol{\Phi}(t_0, t) + \mathcal{G}_c(t_0, t) = \mathcal{G}_c(-\infty, t). \end{aligned} \quad (6)$$

Therefore, in accordance with (6), maximizing (a suitable norm of) $\mathcal{G}_c(-\infty, t)$ is equivalent to minimizing (a suitable norm of) the estimation error covariance $\mathbf{P}(t)$ associated to the LTV system obtained by linearizing the nonlinear system around a nominal trajectory. Consequently, the trajectory $\mathbf{q}(t)$ followed by the robot under the control action resulting from such optimization is expected to provide a state estimate with minimum uncertainty when the linearization (5) around $\mathbf{q}(t)$ is sufficiently representative of the true system (1)-(2). Specifically, a suitable index for expressing the maximum estimation uncertainty is the smallest eigenvalue of the CG ($\lambda_{\min}(\mathcal{G}_c)$), which can be approximated with a differentiable approximation, hereafter named as μ -norm, i.e., $\|\mathcal{G}_c\|_{\mu}$ when two eigenvalues of the GC coalesce (see [11] for details).

Remark 1: The covariance matrix provided by the EKF built on (5) is equal to the inverse of the FIM [20], implying that CG coincides with the FIM in this case. However, the CG remains the measure of constructibility/observability for the original nonlinear system (1)-(2), holding for nonlinear observers as the UKF, in the same way as the observability rank condition for nonlinear systems [1], [2]. In addition, the discrete-time CG is, in turn, a solution to the discrete-time Riccati equation of the EKF and corresponds to the continuous-time CG if $\mathbf{R}_{DT} = \mathbf{R} \Delta T$ with \mathbf{R}_{DT} discretize measurement noise covariance (see [22, p. 232] for further details).

The main difficulty in using the CG is the lack, in most cases, of a closed-form expression of the sensitivity matrix $\boldsymbol{\Phi}(t, t_f)$. Finding a solution for (4) is as complex and costly as finding a solution for (1). Differently from [11], in this letter we further exploit the differential flatness property by feedback linearizing the nonlinear system to transform it in the Brunovsky form, for which the transition matrix reduces to the exponential of a Jordan block. However, our objective is to maximize performance in estimating the original state of the nonlinear system, as it is then used to compute the nonlinear feedback for linearization. Therefore, in the next section, we introduce a methodology to come back to the CG for the original nonlinear system while circumventing the computational cost of numerically retrieving the sensitivity matrix.

III. OPTIMAL INFORMATION-AWARE TRAJECTORY GENERATION VIA FEEDBACK LINEARIZATION

This section first introduces the two main tools employed in our approach: (i) the Brunovsky form for rewriting the CG in terms of the exponential of a Jordan block matrix; (ii) B-spline curve for parameterizing the flat outputs. Then, a novel active sensing control problem is formulated.

A. CG Decomposition via the Brunovsky Form

Let us start by considering the differential flatness definition.

Definition 1 (Differentially Flat Systems [16]): System (1) is differentially flat if there exist flat outputs $\xi = [\xi_1, \dots, \xi_k]^\top = \mathbf{F}_\xi(\mathbf{q}, \mathbf{u}, \dot{\mathbf{u}}, \ddot{\mathbf{u}}, \dots, \mathbf{u}^{(l)}) \in \mathbb{R}^k$ such that the states and inputs can be expressed as $\mathbf{q} = \mathbf{q}(\xi, \dot{\xi}, \dots, \xi^{(l)})$ and $\mathbf{u} = \mathbf{u}(\xi, \dot{\xi}, \dots, \xi^{(l)})$, where l are non-negative integers – without the need to integrate the system.

Example 1 (Unicycle Vehicle Moving on a Plane): Let $\mathbf{q}(t) = (x(t), y(t), \theta(t))$ with $(x(t), y(t))$ the position on the plane and $\theta(t)$ the heading. The robot kinematic is $\dot{\mathbf{q}} = \mathbf{g}_1(\mathbf{q})v + \mathbf{g}_2(\mathbf{q})\omega$ with $\mathbf{g}_1 = [\cos \theta, \sin \theta, 0]^\top$, $\mathbf{g}_2 = [0, 0, 1]^\top$, and v and ω the linear and angular velocities, respectively. The flat output for this case is $\xi = [\xi_1, \xi_2]^\top = [x, y]^\top$, while θ , v and ω can be expressed in terms of ξ , $\dot{\xi}$, and $\ddot{\xi}$ as: $\theta = \arctan(\dot{\xi}_1/\dot{\xi}_2)$, $v = \sqrt{\dot{\xi}_1^2 + \dot{\xi}_2^2}$ and $\omega = (\ddot{\xi}_2\dot{\xi}_1 - \dot{\xi}_1\ddot{\xi}_2)/(\dot{\xi}_1^2 + \dot{\xi}_2^2)$.

Let $r = \sum_{i=1}^k r_i$ be the total relative degree of the system (1) with r_i the relative degree of ξ_i . If $r < n$, then the relative degree of some output is lower than that of others, indicating that some inputs influence the output earlier than others. Therefore, in order to proceed with a feedback linearization, first of all, it is necessary to extend the state of the system (1) by considering as new control inputs the derivative of the inputs in \mathbf{u} with lower relative degree until a finite order [23].

Let $\mathbf{q}_e \in \mathbb{R}^{n_e}$ with $n_e > n$ be the new extended states, \mathbf{u}_e the control inputs of the extended nonlinear system, and the total relative degree of the extended system $r_e = \sum_{i=1}^k r_i = n_e$. Hereafter, we consider that each flat output has the same relative degree \bar{r} , implying $r_e = \kappa\bar{r}$. It is now possible to determine a change of coordinates $\eta = [\xi^\top, \dot{\xi}^\top, \dots, \xi^{(\bar{r}-1)\top}]^\top = \mathbf{F}_\eta(\mathbf{q}_e) \in \mathbb{R}^{n_e}$ for which the new dynamics is

$$\dot{\eta}(t) = \frac{\partial \mathbf{F}_\eta(\mathbf{q}_e)}{\partial \mathbf{q}_e} \dot{\mathbf{q}}_e \Big|_{\mathbf{q}_e = \mathbf{F}_\eta^{-1}(\eta)} = \mathbf{f}_\eta(\eta(t), \mathbf{u}_e(t)) \quad (7)$$

where $\dot{\xi}^{(\bar{r}-1)} = \dot{\xi}^{(\bar{r})} = \mathbf{\Gamma}(\mathbf{q}_e) + \mathbf{E}(\mathbf{q}_e)\mathbf{u}_e \Big|_{\mathbf{q}_e = \mathbf{F}_\eta^{-1}(\eta)}$, $\mathbf{E} \in \mathbb{R}^{k \times \kappa}$, and $\mathbf{\Gamma} \in \mathbb{R}^k$. Values of \mathbf{q}_e such that the inverse of $\mathbf{E}(\cdot)$ does not exist are known as intrinsic flatness singularities [24]. For all the other values of \mathbf{q}_e such that the change of coordinates has no singularity (aka apparent singularities [24]), the static nonlinear feedback $\mathbf{u}_e = -\mathbf{E}^{-1}(\mathbf{q}_e)\mathbf{\Gamma}(\mathbf{q}_e) + \mathbf{E}^{-1}(\mathbf{q}_e)\mathbf{v}$ transforms (7) as

$$\begin{aligned} \dot{\eta}(t) &= \mathbf{A}_b\eta(t) + \mathbf{B}_b\mathbf{v}(t) \\ \mathbf{z}(t) &= \mathbf{h}(\mathbf{F}_\eta^{-1}(\eta)) + \boldsymbol{\mu}(t) \end{aligned} \quad (8)$$

where $\mathbf{v} = \xi^{(\bar{r})} \in \mathbb{R}^k$ are the new fictitious control inputs for the linearized system (8) (to be designed in order to obtain an arbitrary asymptotic convergence to desired values η_d of variables η). Moreover,

$$\mathbf{A}_b = \begin{bmatrix} \mathbf{0}_{\kappa(\bar{r}-1) \times \kappa} & \mathbf{I}_{\kappa(\bar{r}-1) \times \kappa(\bar{r}-1)} \\ \mathbf{0}_{\kappa \times \kappa} & \mathbf{0}_{\kappa \times \kappa(\bar{r}-1)} \end{bmatrix}, \quad \mathbf{B}_b = \begin{bmatrix} \mathbf{0}_{\kappa(\bar{r}-1) \times \kappa} \\ \mathbf{I}_{\kappa \times \kappa} \end{bmatrix}.$$

The noisy outputs $\mathbf{z}(t)$ (still nonlinear) expressed in the new coordinates η are obtained from (2) by using the inverse transformation $\mathbf{F}_\eta^{-1}(\eta)$. Since the outputs remain the same as in (2) and the noise is state-independent, the latter affects the measurements in the new coordinates η as in (2).

Example 2 (Unicycle Vehicle Moving on a Plane): Both flat outputs have relative degree 1 w.r.t. v and relative degree 2 w.r.t. ω . As a consequence, by deriving the flat outputs until a control input appears, we obtain a matrix \mathbf{E} with a null column. By extending the state variable with v , i.e., $\mathbf{q}_e = [x, y, \theta, v]^\top = [q_{e1}, q_{e2}, q_{e3}, q_{e4}]^\top$, and by defining a new control input a , such that $\dot{v} = a$, i.e., $\mathbf{u}_e = [a, \omega]^\top$, one has $\eta = [x, y, \dot{x}, \dot{y}]$, $\mathbf{v} = [\ddot{x}, \ddot{y}]^\top$, $\mathbf{E}(\mathbf{q}_e) = \begin{bmatrix} \cos q_{e3} & -q_{e4} \sin q_{e3} \\ \sin q_{e3} & \cos q_{e3} \end{bmatrix}$ and $\mathbf{\Gamma}(\mathbf{q}_e) = 0$ (see [25] for more details).

The transition matrix of (8) can be computed in closed-form as $\Phi(\tau, t_f) = e^{\mathbf{A}_b(\tau-t_f)}$. Therefore, its CG is

$${}^\eta \mathcal{G}_c(t_0, t_f) = \int_{t_0}^{t_f} e^{\mathbf{A}_b^\top(\tau-t_f)} \mathbf{H}_\eta^\top \mathbf{R}^{-1}(t) \mathbf{H}_\eta e^{\mathbf{A}_b(\tau-t_f)} dt \quad (9)$$

where $\mathbf{H}_\eta = \frac{\partial \mathbf{h}}{\partial \eta} = \frac{\partial \mathbf{h}}{\partial \mathbf{q}} \frac{\partial \mathbf{q}}{\partial \eta}$. Moreover, similarly to (6), ${}^\eta \mathcal{G}_c(-\infty, t_f)$ can be usefully decomposed as

$${}^\eta \mathcal{G}_c(-\infty, t_f) = \Phi(t, t_f)^\top {}^\eta \mathcal{G}_c(-\infty, t) \Phi(t, t_f) + {}^\eta \mathcal{G}_c(t, t_f)$$

implying

$${}^\eta \mathcal{G}_c(-\infty, t) = \mathbf{P}_\eta^{-1}(t). \quad (10)$$

However, it should be noted that (9) quantifies the amount of information about the *flat outputs* and their derivatives until a finite order, while in practice one is usually interested in the original variable \mathbf{q} of system (1)–(2), especially because \mathbf{q} is used to compute the feedback control law \mathbf{u}_e . It also does not consider the information contained in the nonlinearity of \mathbf{u}_e . In the following, we will show how to address both problems. Let us start again from system (7). The covariance matrix \mathbf{P}_{q_e} of the extended state \mathbf{q}_e can be expressed in terms of the covariance matrix \mathbf{P}_η of the state η , through the following approximation [22, p. 438]:

$$\mathbf{P}_{q_e} \approx \mathbf{J}_\eta \mathbf{P}_\eta \mathbf{J}_\eta^\top \quad (11)$$

where $\mathbf{J}_\eta = \frac{\partial \mathbf{F}_\eta^{-1}(\eta)}{\partial \eta}$ is the Jacobian of the inverse flatness transformation $\mathbf{F}_\eta^{-1}(\eta) = \mathbf{q}_e$. Notice that, if \mathbf{P}_η was the exact covariance matrix of η , (11) would hold exactly in case $\mathbf{F}_\eta(\cdot)$ is linear.

Proposition 1: Let us consider the nonlinear system (7). The amount of information about variables \mathbf{q}_e encoded by ${}^{q_e} \mathcal{G}_c$ can be retrieved from ${}^\eta \mathcal{G}_c$ through the following expression:

$$\begin{aligned} {}^{q_e} \mathcal{G}_c(-\infty, t_f) &= \mathbf{J}_\eta^{-\top}(t_f) (\Phi_\eta^\top(t, t_f) {}^\eta \mathcal{G}_c(-\infty, t) \Phi_\eta(t, t_f) \\ &\quad + {}^\eta \mathcal{G}_c(t, t_f)) \mathbf{J}_\eta^{-1}(t_f), \end{aligned} \quad (12)$$

where $\Phi_\eta(t, t_f)$ is the state transition matrix of (7).

Proof: Let us consider the inverse of (11) defined as $\mathbf{P}_{q_e}^{-1} \approx \mathbf{J}_\eta^{-\top} \mathbf{P}_\eta^{-1} \mathbf{J}_\eta^{-1}$. By exploiting the equality (10) and by substituting the CG decomposition to ${}^\eta \mathcal{G}_c(-\infty, t)$, i.e., (6), then (12) follows. ■

Notice that, the CG for the original system (1)–(2), i.e., ${}^q \mathcal{G}_c(-\infty, t_f)$, is a submatrix of ${}^{q_e} \mathcal{G}_c(-\infty, t_f)$. Proposition 1 cannot be extended to (8) as it is obtained by a nonlinear feedback. A possible way to recover the nonlinearity contained in the input transformation from \mathbf{u}_e to \mathbf{v} , is to further extend \mathbf{q}_e by adding control \mathbf{u}_e among the state variables, obtaining $\mathbf{q}'_e = [\mathbf{q}_e^\top, \mathbf{u}_e^\top]^\top$. The new change of coordinates

is $\eta_e = [\eta^\top, \mathbf{v}^\top]^\top = \mathbf{F}_{\eta_e}(\mathbf{q}'_e) = [\mathbf{F}_\eta(\mathbf{q}_e)^\top, (\mathbf{E}(\mathbf{q}_e)\mathbf{u}_e + \mathbf{\Gamma}(\mathbf{q}_e))^\top]^\top$ and the new static nonlinear feedback becomes $\mathbf{u}'_e = -\mathbf{E}_e^{-1}(\mathbf{q}'_e)\mathbf{\Gamma}_e(\mathbf{q}'_e) + \mathbf{E}_e^{-1}(\mathbf{q}'_e)\mathbf{v}_e$ where $\mathbf{v}_e = \dot{\mathbf{v}} \in \mathbb{R}^\kappa$ is the new fictitious control input. The dynamics of the system with state η_e and input \mathbf{v}_e is

$$\begin{aligned} \dot{\eta}_e(t) &= \mathbf{A}_{b_e}\eta_e(t) + \mathbf{B}_{b_e}\mathbf{v}_e(t) \\ \mathbf{z}(t) &= \mathbf{h}(\mathbf{F}_\eta^{-1}(\eta)) + \boldsymbol{\mu}(t), \end{aligned} \quad (13)$$

with

$$\begin{aligned} \mathbf{A}_{b_e} &= \begin{bmatrix} \mathbf{A}_b & \mathbf{A}_b^* \\ \mathbf{0}_{\kappa \times n_e} & \mathbf{0}_{\kappa \times \kappa} \end{bmatrix}, \mathbf{B}_{b_e} = \begin{bmatrix} \mathbf{0}_{n_e \times \kappa} \\ \mathbf{I}_{\kappa \times \kappa} \end{bmatrix}, \\ \mathbf{A}_{b_e}^* &= \begin{bmatrix} \mathbf{0}_{\kappa(\bar{\nu}-1) \times \kappa} \\ \mathbf{I}_{\kappa \times \kappa} \end{bmatrix}, \end{aligned}$$

where $\mathbf{A}_{b_e}^*$ captures the effect of the state added to recover the nonlinearity of the input transformation.

Example 3 (Unicycle Vehicle Moving on a Plane): The state of the augmented system (13) is composed of $\eta_e = [\eta^\top, \mathbf{v}^\top]^\top$ and $\mathbf{v}_e = [\ddot{x}, \ddot{y}]^\top$. Consequently, $\mathbf{q}'_e = [\mathbf{q}_e^\top, a, \omega]^\top = [q'_{e1}, q'_{e2}, q'_{e3}, q'_{e4}, q'_{e5}, q'_{e6}]^\top$, $\mathbf{u}'_e = [\dot{a}, \dot{\omega}]^\top$. By computing the jerk of the flat outputs, we obtain $\mathbf{E}_e(\mathbf{q}'_e) = \begin{bmatrix} \cos q'_{e3} & -q'_{e4} \sin q'_{e3} \\ \sin q'_{e3} & \cos q'_{e3} \end{bmatrix}$ and $\mathbf{\Gamma}_e(\mathbf{q}'_e) = \begin{bmatrix} -q'_{e6}q'_{e5} \sin q'_{e3} - q'_{e4}q'_{e6} \cos q'_{e3} \\ 2q'_{e6}q'_{e5} \cos q'_{e3} + q'_{e4}q'_{e6} \sin q'_{e3} \end{bmatrix}$ (similar findings can be observed in [26]).

Proposition 2: Let us consider (13) with $\mathbf{v}_e = \mathbf{E}_e(\mathbf{q}'_e)\mathbf{u}'_e + \mathbf{\Gamma}_e(\mathbf{q}'_e)|_{\mathbf{q}'_e=\mathbf{F}_\eta^{-1}(\eta_e)}$ and its transition matrix $\Phi_{\eta_e}(t, t_f)$. The state transition matrix of system (8) is a submatrix of $\Phi_{\eta_e}(t, t_f)$ defined as

$$\Phi_\eta(t, t_f) = e^{\mathbf{A}_b(t-t_f)} + \mathbf{Y}(t)\mathbf{Z}(\eta(t_f)) \quad (14)$$

with

$$\mathbf{Y}(t) = \left(\int_0^{t-t_f} e^{\mathbf{A}_b(t-t_f-\tau)} d\tau \right) \mathbf{A}_b^* \quad (15)$$

$$\begin{aligned} \mathbf{Z}(\eta(t_f)) &= \frac{\partial}{\partial \eta(t_f)} \left(-\mathbf{E}^{-1}(\mathbf{F}_\eta^{-1}(\eta(t_f)))\mathbf{\Gamma}(\mathbf{F}_\eta^{-1}(\eta(t_f))) \right. \\ &\quad \left. + \mathbf{E}^{-1}(\mathbf{F}_\eta^{-1}(\eta(t_f)))\mathbf{v} \right) \end{aligned} \quad (16)$$

where $\mathbf{Y}(t)$ and $\mathbf{Z}(\eta(t_f))$ model the effects of the input on η .

Proof: Let us consider the transition matrix of (13) with $\mathbf{v}_e = \mathbf{E}_e(\mathbf{q}'_e)\mathbf{u}'_e + \mathbf{\Gamma}_e(\mathbf{q}'_e)|_{\mathbf{q}'_e=\mathbf{F}_\eta^{-1}(\eta_e)}$. One has

$$\begin{aligned} \Phi_{\eta_e}(t, t_0) &= e^{\mathbf{A}_{b_e}(t-t_0)} + \\ &\quad + \frac{\partial}{\partial \eta_0} \int_{t_0}^t \mathbf{B}_{b_e}\mathbf{E}_e(\mathbf{q}'_e)\mathbf{u}'_e + \mathbf{\Gamma}_e(\mathbf{q}'_e)|_{\mathbf{q}'_e=\mathbf{F}_\eta^{-1}(\eta_e)} d\tau, \end{aligned} \quad (17)$$

with

$$e^{\mathbf{A}_{b_e}(t-t_0)} = \begin{pmatrix} e^{\mathbf{A}_b(t-t_0)} & \mathbf{Y}(t) \\ \mathbf{0}_{\kappa \times n_e} & \mathbf{I}_{\kappa \times \kappa} \end{pmatrix}.$$

the transition matrix of (21) (see [27, p. 215] for its derivation). Let us compute now the state transition matrix of the system with state \mathbf{q}'_e as a function of η_e

$$\begin{aligned} \Phi_{q'_e}(t, t_0) &= \frac{\partial \mathbf{q}_e}{\partial \mathbf{q}_{e0}} = \frac{\partial \mathbf{q}_e}{\partial \eta_e} \Phi_{\eta_e}(t, t_0) \frac{\partial \eta_{e0}}{\partial \mathbf{q}_{e0}} \\ &= \mathbf{J}_{\eta_e} \Phi_{\eta_e}(t, t_0) \mathbf{J}_{\eta_{e0}}^{-1}, \end{aligned} \quad (18)$$

where $\mathbf{J}_{\eta_e} = \frac{\partial \mathbf{q}_e}{\partial \eta_e} = \frac{\partial \mathbf{F}_\eta^{-1}(\eta_e)}{\partial \eta_e}$ is the Jacobian of the inverse flatness change of coordinates $\mathbf{F}_\eta^{-1}(\eta_e) = [\mathbf{F}_\eta(\eta)^{-\top}, (-\mathbf{E}^{-1}(\mathbf{q}_e)\mathbf{\Gamma}(\mathbf{q}_e) + \mathbf{E}^{-1}(\mathbf{q}_e)\mathbf{v})^\top]^\top|_{\mathbf{q}_e=\mathbf{F}_\eta^{-1}(\eta)} = \mathbf{q}'_e$. As a consequence,

$$\mathbf{J}_{\eta_e} = \begin{pmatrix} \mathbf{J}_\eta & \mathbf{0}_{n_e \times \kappa} \\ \mathbf{Z}(\eta) & \mathbf{E}^{-1}(\mathbf{F}_\eta^{-1}(\eta)) \end{pmatrix}.$$

with $\mathbf{Z}(\eta)$ obtained from (16) at a generic time t . Of course, in (18), $\mathbf{J}_{\eta_{e0}}^{-1}$ is the inverse of \mathbf{J}_{η_e} evaluated at the initial state η_{e0} . By replacing (17) in (18) and after some algebra,

$$\Phi_{q'_e}(t, t_0) = \begin{pmatrix} \mathbf{J}_\eta(e^{\mathbf{A}_b(t-t_0)} + \mathbf{Y}(t)\mathbf{Z}(\eta_0))\mathbf{J}_{\eta_0}^{-1} & * \\ * & * \end{pmatrix} \quad (19)$$

From (19), it is possible to extract the transition matrix

$$\Phi_{q_e} = \mathbf{J}_\eta(e^{\mathbf{A}_b(t-t_0)} + \mathbf{Y}(t)\mathbf{Z}(\eta_0))\mathbf{J}_{\eta_0}^{-1}, \quad (20)$$

i.e., the state transition matrix of \mathbf{q}_e obtained as an exact coordinates change. Finally, from (20) and (18) the thesis follows. ■

We are now ready to state the main result of this letter, i.e., retrieving in closed-form the CG of the original nonlinear system (1)-(2) by exploiting Propositions 1 and 2.

Proposition 3: Let us consider a nonlinear system (1)-(2). Its CG (${}^q\mathcal{G}_c(-\infty, t_f)$) can be computed starting from the CG of (8) as a submatrix of

$$\begin{aligned} {}^q\mathcal{G}_c(-\infty, t_f) &= \mathbf{J}_\eta^{-\top}(t_f) \left(\left(e^{\mathbf{A}_b(t-t_f)} + \mathbf{Y}(t)\mathbf{Z}(\eta(t_f)) \right)^\top \right. \\ &\quad \left. {}^\eta\mathcal{G}_c(-\infty, t) \left(e^{\mathbf{A}_b(t-t_f)} + \mathbf{Y}(t)\mathbf{Z}(\eta(t_f)) \right) + \right. \\ &\quad \left. + {}^\eta\mathcal{G}_c(t, t_f) \right) \mathbf{J}_\eta^{-1}(t_f). \end{aligned} \quad (21)$$

Proof: The thesis can be trivially obtained by replacing (14) (thesis of Proposition 2) into the expression (12) (thesis of Proposition 1). ■

Using (21) to maximize a specific norm of ${}^q\mathcal{G}_c(-\infty, t_f)$ effectively enhances the estimation accuracy of the original states \mathbf{q} . A significant advantage of this formulation is the closed-form derivation of all matrices involved in (21), the evaluation of the integral in ${}^\eta\mathcal{G}_c(t, t_f)$ being the only numerical computation to be carried out. Furthermore, if an EKF is employed as an observer, ${}^\eta\mathcal{G}_c(-\infty, t)$ can be obtained as the inverse of the provided covariance matrix. Otherwise, it can be obtained by integrating (21) along the state estimate. Starting from the estimate $\hat{\eta}$ of η , the estimate $\hat{\mathbf{q}}(t)$ of the original variable \mathbf{q} and its covariance matrix $\mathbf{P}_q(t)$ can be determined from $\mathbf{q}_e = \mathbf{F}_\eta(\eta)$ and (11). This reduction in computational complexity significantly increases the practical feasibility of the methodology proposed in [11] to all differentially flat robotics systems.

B. B-Spline Parametrization

As in [11], we adopt B-Splines as parametric curves for the flat outputs. B-Spline curves are linear combinations, through a finite number of L control points $\mathbf{x}_c = (\mathbf{x}_{c,1}^T, \mathbf{x}_{c,2}^T, \dots, \mathbf{x}_{c,L}^T)^T \in \mathbb{R}^{\kappa \cdot L}$, of basis functions $B_j^\alpha : \mathcal{S} \rightarrow \mathbb{R}$ for $j = 1, \dots, L$ obtained by the Cox-de Boor recursion formula. Each B-Spline can be expressed as $\gamma(\mathbf{x}_c, \cdot) : \mathcal{S} \rightarrow \mathbb{R}^\kappa$, $s \mapsto$

$\sum_{j=1}^L \mathbf{x}_{c,j} B_j^\alpha(s, s) = \mathbf{B}_s(s) \mathbf{x}_c$, where \mathcal{S} is a compact subset of \mathbb{R} . The degree of the basis functions α and the sequence of knots $s = (s_1, s_2, \dots, s_\ell)$ are fixed parameters. Moreover, $\mathbf{B}_s(s) \in \mathbb{R}^{k \times L}$ denotes the collection of basis functions, and B_j^α indicates the evaluation of the j -th basis function at s . Additionally, the value $s(t)$ of parameter s , corresponding to time t , can be chosen depending on the desired timing law along the trajectory. Hereafter, an arc-length parametrization is adopted, allowing $s(t)$ to be determined by integrating $\dot{s}(t) = v(\mathbf{x}_c, s)^{-1}$, where $s(t)$ corresponds to the path length t . By parameterizing the flat outputs $F_\xi(\mathbf{q})$ with a B-spline curve $\gamma(\mathbf{x}_c, s)$, all quantities involved in our optimal control strategy (states \mathbf{q} , inputs \mathbf{u} , and any quantity needed for the CG computation) can be expressed as functions of the parameter s (the position along the spline) and the control points \mathbf{x}_c . Consequently, the control points \mathbf{x}_c will be the sole optimization variables. In the following, we denote the state \mathbf{q} and inputs \mathbf{u} determined by the planned B-spline path $\gamma(\mathbf{x}_c, s)$, via the coordinate and input transformation, as $\mathbf{q}_\gamma(\mathbf{x}_c, s)$ and $\mathbf{u}_\gamma(\mathbf{x}_c, s)$.

C. Control Problem Formulation

In this section, we state our optimal active sensing control problem that exploits the differentially flatness property of a nonlinear system as stated in Proposition 3. Let $s_0 = s(t_0)$, $s_f = s(t_f)$ and, in general, $s(t) = s_t$, similarly to [11], the goal is now to solve the following optimization problem

Problem 1 (Optimal Active Sensing Control for Differentially Flat Systems): For all $t \in [t_0, t_f]$, find the optimal location of the control points

$$\begin{aligned} \mathbf{x}_c^*(t) &= \arg \max_{\mathbf{x}_c} \|\mathcal{G}_c(-\infty, t)\|_\mu, \\ \text{with } t &= \int_0^{s_t} v(\sigma, \mathbf{x}_c) d\sigma, \quad v(s, \mathbf{x}_c) = \left\| \frac{d\gamma(s, \mathbf{x}_c)}{ds} \right\|_2, \\ \text{s.t.} \quad & \\ & 1) \hat{\mathbf{q}}(t) - \mathbf{q}_\gamma(\mathbf{x}_c(t), s_t) \equiv \mathbf{0}, \\ & 2) \mathbf{fl}(\mathbf{x}_c(\tau), s_\tau) \neq \mathbf{0}, \quad \forall \tau \in [t, t_f] \\ & 3) \underline{\mathbf{q}} \leq \mathbf{q}_\gamma(\mathbf{x}_c(t), s_t) \leq \bar{\mathbf{q}} \\ & 4) \underline{\mathbf{u}} \leq \mathbf{u}_\gamma(\mathbf{x}_c(t), s_t) \leq \bar{\mathbf{u}} \end{aligned}$$

where $\mathcal{G}_c(-\infty, t)$ is computed as in Proposition 3, 1) is the state coherency for maintaining the B-Spline trajectory passing through the current state estimation value provided online by the employed observer, 2) avoids intrinsic singularities, ensuring the existence of a feedback-linearizing control law (see [11] for details), 3) and 4) replace the energy constraint in [11] for the well-posedness of the optimization problem.

Problem 1 is solved using the CasADi tool [28] with a direct single shooting method by adopting the ma57 ipopt solver. We have rewritten the control problem as a NonLinear Program (NLP) problem where \mathbf{x}_c^* is found through a gradient descent method. Moreover, a 4th-order Runge-Kutta method is employed for the computation of $\mathcal{G}_c(t, t_f)$ with sampling time ΔT . Furthermore, the control problem complexity can be approximated as $\mathcal{O}(\alpha \times \mathbf{x}_c \times N)$ with $N = \frac{T}{\Delta T}$, T being the simulation time.

IV. RESULTS

We test the proposed approach with a unicycle vehicle and a planar quadrotor. We statistically compare the estimation performance corresponding to random paths, also used as initial guess for Problem 1, to the results obtained by solving the problem defined in [11], referred to as AS (acronym for *Active Sensing*) paths, and Problem 1, referred to as AS-FL (acronym for *Active Sensing with Feedback Linearization*) paths. Both optimization problems are solved offline. An EKF is used for state estimation when both the random paths and the AS paths are tested. For the AS-FL, an EKF is still used but the prediction step builds on a *linear* process model.

Case A - Unicycle vehicle. The system is equipped with a range sensor providing distance measurements w.r.t. two fixed markers, i.e., $z_i = \sqrt{(x - x_{M_i})^2 + (y - y_{M_i})^2}$ where (x_{M_i}, y_{M_i}) is the i -th marker position in the Cartesian space with $i = 1, 2$. The positions of the markers are (0, 0)m and (0, 5)m. We generated 100 random paths. For each simulation, $\mathbf{q}_0 = [14 \text{ m}, 1 \text{ m}, -\pi \text{ rad}]^\top$ while $\hat{\mathbf{q}}_0$ is generated from \mathbf{q}_0 by $\mathbf{P}_0 = \text{diag}([0.1, 0.1, 0.05])$. The input limitations are $0 \leq v \leq 4 \text{ m/s}$ and $-1 \leq \omega \leq 1 \text{ rad/s}$, the bounds on the state are $0 \leq x, y \leq 15 \text{ m}$, while θ is not bounded. The simulation time is $T = 10\text{s}$, and the sampling time is $\Delta T = 0.1\text{s}$. Moreover, we assume a white Gaussian output noise with covariance matrix $\mathbf{R} = 0.1\mathbf{I}$. Finally, we consider a B-spline with degree $\alpha = 2$ and $L = 6$ control points. For each optimized path, the smallest eigenvalue of $\mathbf{P}^{-1}(t_f)$ and the Root Mean Square of the estimation error at the final time, i.e., $\text{RMS}(e_f)$, are considered. Their average values and standard deviations are computed and a statistical analysis is provided by using a Wilcoxon rank sum test. A significance level of 5% was assumed and p-values less than 10^{-4} were considered equal to zero. The statistical results are shown in Fig. 1(a), proving that the AS-FL exhibits slightly different statistical properties concerning uncertainty and estimation errors when compared to AS. However, when comparing both AS and AS-FL approaches to the random one, the p-values are zero, meaning that both provide paths with the same information content. Moreover, finding the optimal solution for AS-FL requires a shorter time, confirming the beneficial effect of the proposed method.

Case B - Planar Quadrotor. Let $\mathbf{q} = [x, y, \dot{x}, \dot{y}, \theta, \omega]^\top = [\mathbf{p}, \mathbf{v}, \theta, \omega]^\top$ be the state of the planar quadrotor and let $\mathbf{u} = [f, \tau]^\top$ be the inputs consisting of the total thrust and torque. The system dynamic is the same as in [11, eq. (31)]. The same outputs z_i , $i = 1, 2$, as for the unicycle are considered. We generated 10 random paths. For each simulation, $\mathbf{q}_0 = [10 \text{ m}, 1 \text{ m}, 0 \text{ m/s}, 0 \text{ m/s}, 0 \text{ rad}, 0 \text{ rad/s}]^\top$ while $\hat{\mathbf{q}}_0$ by using $\mathbf{P}_0 = \text{diag}([0.1, 0.1, 0.01, 0.01, 0.01, 0.01])$. The input limits are $4 \leq f \leq 7 \text{ N}$ and $-1 \leq \tau \leq 1 \text{ Nm}$. Moreover, $T = 10\text{s}$, $\Delta T = 0.1\text{s}$, and $\mathbf{R} = 0.1\mathbf{I}$. The B-spline has a degree $\alpha = 4$ and $L = 8$ control points. The statistical results are shown in Fig. 1(b). Also, in this case, AS-FL and AS present the same statistical properties in terms of RMS and collected information. However, compared to random paths they provide a more informative path. Moreover, the computational time is smaller for AS-FL, in spite of the increased complexity w.r.t. previous case.

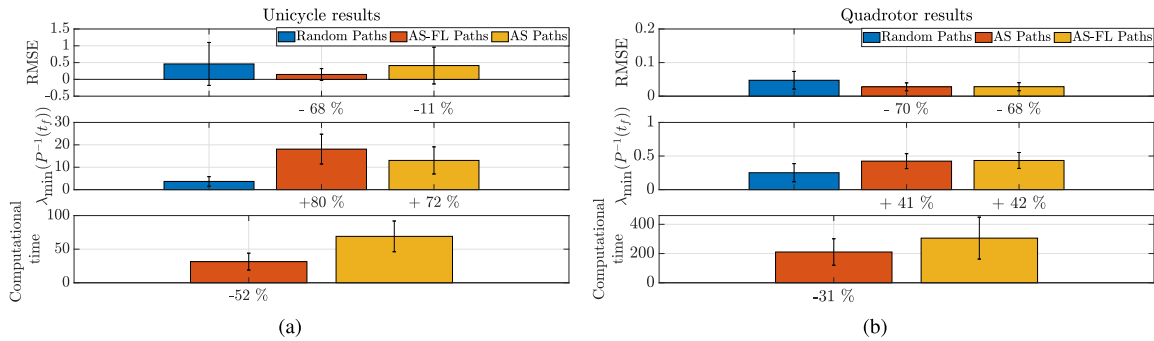


Fig. 1. Statistical results for the unicycle vehicle (a) and planar quadrotor (b): average RMS of estimation errors with standard deviations, and percentage improvement of AS-FL and AS w.r.t. random paths; average $\lambda_{\min}(P^{-1}(t_f))$ with standard deviations, and percentage improvement of AS-FL and AS w.r.t. the random paths; average computational time with standard deviation, and percentage improvement of the AS-FL w.r.t. the AS.

V. CONCLUSION AND FUTURE WORKS

We have introduced an active sensing control methodology exploiting flatness to transform the nonlinear system in the Brunovsky form, thus ensuring a closed-form computation of the transition matrix which appears in the CG and significantly reducing the computational load of the optimization problem. Our methodology has shown substantial improvements in computational time and estimation performance. Future works will address the online implementation, real experiments, and the release of an open-source AS/AS-FL code, as well as the link of CG with nonlinear observers (UKF).

REFERENCES

- [1] R. Hermann and A. J. Krener, "Nonlinear controllability and observability," *IEEE Trans. Autom. Control*, vol. 22, no. 5, pp. 728–740, Oct. 1977.
- [2] A. J. Krener and K. Ide, "Measures of unobservability," in *Proc. IEEE Conf. Decision Control (CDC) Chin. Control Conf. (CCC)*, 2009, pp. 6401–6406.
- [3] A. Bicchi, D. Prattichizzo, A. Marigo, and A. Balestrino, "On the observability of mobile vehicle localization," in *Theory and Practice of Control and Systems*. Singapore: World Sci., 1998, pp. 142–147.
- [4] M. Sun, A. Gaggari, P. Trautman, and T. Murphey, "Fast ergodic search with kernel functions," 2024, *arXiv:2403.01536*.
- [5] S. Koga, A. Asgharivaskasi, and N. Atanasov, "Active exploration and mapping via iterative covariance regulation over continuous SE(3) trajectories," in *Proc. IEEE/RSJ Int. Conf. Intell. Robots Syst. (IROS)*, 2021, pp. 2735–2741.
- [6] S. Rahman and S. L. Waslander, "Uncertainty-constrained differential dynamic programming in belief space for vision based robots," *IEEE Robot. Autom. Lett.*, vol. 6, no. 2, pp. 3112–3119, Apr. 2021.
- [7] J. Shan and Q. Sun, "Observability analysis and optimal information gathering of mobile robot navigation system," in *Proc. IEEE Int. Conf. Inf. Autom.*, 2015, pp. 731–736.
- [8] B. Du, K. Qian, C. Claudel, and D. Sun, "Parallelized active information gathering using Multisensor network for environment monitoring," *IEEE Trans. Control Syst. Technol.*, vol. 30, no. 2, pp. 625–638, Mar. 2022.
- [9] J. Ott, E. Balaban, and M. J. Kochenderfer, "Sequential Bayesian optimization for adaptive informative path planning with multimodal sensing," 2022, *arXiv:2209.07660*.
- [10] P. Tokekar, J. Vander Hook, and V. Isler, "Active target localization for bearing based robotic telemetry," in *Proc. IEEE/RSJ Int. Conf. Intell. Robots Syst.*, 2011, pp. 488–493.
- [11] P. Salaris, M. Cognetti, R. Spica, and P. R. Giordano, "Online optimal perception-aware trajectory generation," *IEEE Trans. Robot.*, vol. 35, no. 6, pp. 1307–1322, Dec. 2019.
- [12] S. Candido and S. Hutchinson, "Minimum uncertainty robot navigation using information-guided POMDP planning," in *Proc. IEEE Int. Conf. Robot. Autom.*, 2011, pp. 6102–6108.
- [13] O. Napolitano, D. Fontanelli, L. Pallottino, and P. Salaris, "Gramian-based optimal active sensing control under intermittent measurements," in *Proc. IEEE Int. Conf. Robot. Autom. (ICRA)*, 2021, pp. 9680–9686.
- [14] M. Cognetti, P. Salaris, and P. Robuffo Giordano, "Optimal active sensing with process and measurement noise," in *Proc. IEEE Int. Conf. Robot. Autom. (ICRA)*, 2018, pp. 2118–2125.
- [15] K. Fritzsche, K. Rößenack, and Y. Guo, "Flat input based canonical form observers for non-integrable nonlinear systems," *Syst. Theory, Control Comput. J.*, vol. 2, no. 1, pp. 13–21, 2022.
- [16] L. Beaver and A. A. Malikopoulos, "Optimal control of differentially flat systems is surprisingly easy," *Automatica*, vol. 159, Jan. 2024, Art. no. 111404.
- [17] M. Tognon and A. Franchi, "Dynamics, control, and estimation for aerial robots tethered by cables or bars," *IEEE Trans. Robot.*, vol. 33, no. 4, pp. 834–845, Aug. 2017.
- [18] M. Tognon, B. Yüksel, G. Buondonno, and A. Franchi, "Dynamic decentralized control for protocentric aerial manipulators," in *Proc. IEEE Int. Conf. Robot. Autom. (ICRA)*, 2017, pp. 6375–6380.
- [19] G. G. Rigatos, "A derivative-free Kalman filtering approach to state estimation-based control of nonlinear systems," *IEEE Trans. Ind. Electron.*, vol. 59, no. 10, pp. 3987–3997, Oct. 2012.
- [20] J. H. Taylor, "The cramer-Rao estimation error lower bound computation for deterministic nonlinear systems," *IEEE Trans. Autom. Control*, vol. 24, no. 2, pp. 343–344, Apr. 1979.
- [21] A. Gelb, *Applied Optimal Estimation*. A. Gelb, J. F. Kasper, R. A. Nash, C. F. Price, and A. A. Sutherland, Eds. Cambridge, MA: MIT Press, 1974.
- [22] D. Simon, *Optimal State Estimation: Kalman, H Infinity, and Nonlinear Approaches*. Hoboken, NJ, USA: Wiley, 2006.
- [23] A. Isidori, C. H. Moog, and A. D. Luca, "A sufficient condition for full linearization via dynamic state feedback," in *Proc. IEEE Conf. Decision Control (CDC)*, 1986, pp. 203–208.
- [24] Y. J. Kaminski, J. Lévine, and F. Ollivier, "Intrinsic and apparent singularities in differentially flat systems, and application to global motion planning," *Syst. Control Lett.*, vol. 113, pp. 117–124, Mar. 2018.
- [25] G. Oriolo, A. De Luca, and M. Vendittelli, "WMR control via dynamic feedback linearization: Design, implementation, and experimental validation," *IEEE Trans. Control Syst. Technol.*, vol. 10, no. 6, pp. 835–852, Nov. 2002.
- [26] E. Yang, D. Gu, T. Mita, and H. Hu, "Nonlinear tracking control of a car-like mobile robot via dynamic feedback linearization," in *Proc. Control Conf.*, 2004, pp. 1–5. [Online]. Available: <https://api.semanticscholar.org/CorpusID:6857583>
- [27] R. A. DeCarlo, *Linear Systems: A State Variable Approach with Numerical Implementation*. Upper Saddle River, NJ, USA: Prentice-Hall, 1989.
- [28] J. Andersson, "A general-purpose software framework for dynamic optimization," Ph.D. dissertation, Arenberg Doctoral School, KU Leuven, Leuven, Belgium, 2013.